

PAPER

Phase transitions in huddling emperor penguins

To cite this article: S Richter *et al* 2018 *J. Phys. D: Appl. Phys.* **51** 214002

View the [article online](#) for updates and enhancements.

Related content

- [Particulate matter concentration mapping from MODIS satellite data: a Vietnamese case study](#)
Thanh T N Nguyen, Hung Q Bui, Ha V Pham *et al.*
- [Structural organisation and dynamics in king penguin colonies](#)
Richard Gerum, Sebastian Richter, Ben Fabry *et al.*
- [Simulating the Refractive Index Structure Constant \$\{\(C\) \cdot \{n\}^{\{2\}}\}\$ in the Surface Layer at Antarctica with a Mesoscale Model](#)
Chun Qing, Xiaoqing Wu, Xuebin Li *et al.*



IOP | ebooks™

Bringing you innovative digital publishing with leading voices to create your essential collection of books in STEM research.

Start exploring the collection - download the first chapter of every title for free.

Phase transitions in huddling emperor penguins

S Richter^{1,2}, R Gerum¹, A Winterl¹, A Houstin^{3,4}, M Seifert¹, J Peschel¹, B Fabry¹, C Le Bohec^{3,4} and D P Zitterbart^{1,2}

¹ Biophysics Group, Friedrich-Alexander University, Erlangen, Germany

² Applied Ocean Physics and Engineering, Woods Hole Oceanographic Institution, Woods Hole, MA 02543, United States of America

³ Département de Biologie Polaire, Monaco, Centre Scientifique de Monaco, Principality of Monaco

⁴ Université de Strasbourg, CNRS, IPHC, UMR 7178, Strasbourg, France

E-mail: sebastian.sr.richter@gmail.com (S Richter)

Received 21 February 2018, revised 27 March 2018

Accepted for publication 4 April 2018

Published 2 May 2018



Abstract

Emperor penguins (*Aptenodytes forsteri*) are highly adapted to the harsh conditions of the Antarctic winter: they are able to fast for up to 134 days during breeding. To conserve energy, emperor penguins form tight groups (huddles), which is key for their reproductive success. The effect of different meteorological factors on the huddling behaviour, however, is not well understood. Using time-lapse image recordings of an emperor penguin colony, we show that huddling can be described as a phase transition from a fluid to a solid state. We use the colony density as order parameter, and an apparent temperature that is perceived by the penguins as the thermodynamic variable. We approximate the apparent temperature as a linear combination of four meteorological parameters: ambient temperature, wind speed, global radiation and relative humidity. We find a wind chill factor of $-2.9\text{ °C (ms}^{-1}\text{)}^{-1}$, a humidity chill factor of $-0.5\text{ °C/\% rel. humidity}$, and a solar radiation heating factor of $0.3\text{ °C (Wm}^{-2}\text{)}^{-1}$. In the absence of wind, humidity and solar radiation, the phase transition temperature (50% huddling probability) is -48.2 °C for the investigated time period (May 2014). We propose that higher phase transition temperatures indicate a shrinking thermal insulation and thus can serve as a proxy for lower energy reserves of the colony, integrating pre-breeding foraging success at sea and energy expenditure at land due to environmental conditions. As current global change is predicted to have strong detrimental effects on emperor penguins within the next decades, our approach may thus contribute towards an urgently needed long-term monitoring system for assessing colony health.

Keywords: collective behaviour, phase transition, emperor penguin, huddling, climate variability, environmental conditions

 Supplementary material for this article is available [online](#)

(Some figures may appear in colour only in the online journal)

Introduction

Emperor penguins (*Aptenodytes forsteri*) breed during the Antarctic winter and survive temperatures below -50 °C and wind speeds exceeding 150 km h^{-1} . The male penguins fast for up to 134 days (Prévost 1961, Isenmann 1971) during mating and incubation until the females return from foraging.

Therefore, the conservation of energy is critical for successfully incubating the unique egg until hatching. A key component for energy conservation is the formation of huddles (Le Maho 1977, Gilbert *et al* 2010), which are constantly reorganized to minimize energy loss (Zitterbart *et al* 2011, Gerum *et al* 2013). Huddles are densely packed groups of individuals that allow the colony to share body heat, reduce

effective surface area, and shelter each other from the wind. Temperatures inside a huddle can reach up to 37.5 °C (Gilbert *et al* 2006). Previous studies reported that the likelihood of huddling increases with lower temperature and higher wind speed (Gilbert *et al* 2006, 2008), and with lower solar radiation (Ancel *et al* 2015).

The rearrangement of the colony structure during huddle formation is reminiscent of a phase transition in non-living matter. A phase transition in the context of an Emperor penguin colony describes the change between a solid state—corresponding to a dense huddle—and a liquid or gaseous state—corresponding to a loose configuration of individual penguins—in response to one or more external parameters (Canals and Bozinovic 2011, Vicsek and Zafeiris 2012) such as temperature, wind speed or solar radiation (figure 1).

In this study, we apply the concept of a phase transition to a penguin colony and study their huddling behaviour in response to short-term fluctuations of the following environmental parameters: ambient temperature, wind speed, relative humidity, and global solar radiation. We use the density of the colony as order parameter of the system to describe the phase, or state, of the colony. Density is extracted from time-lapse image recordings of an emperor penguin colony at Pointe Géologie, Antarctica (66°39'46.5"S 140°00'14.1"E). We define an ‘apparent temperature’ perceived by the penguins as a linear combination of the ambient temperature, wind speed (times a wind chill factor), relative humidity (times a humidity chill factor), and solar radiation (times a solar heating factor). We then model the colony state as a function of the apparent temperature, whereby we fit the influence of wind chill, humidity chill, and solar heating, and the range and transition point of the apparent temperature over which the phase transition occurs.

Material & methods

Data acquisition

We acquired time lapse photography recordings of the Pointe Géologie emperor penguin colony, adjacent to the French Antarctic research station Dumont d’Urville (66°39'46.5"S 140°00'14.1"E, figures 2(a) and (b)). Images are recorded by a mobile observatory (*micrObs*) over multiple days or weeks at frame rates of up to 1 frame per second (figure 2(c)).

We use a Panasonic DMC-G5 digital single lens mirrorless (DSLM) camera equipped with a 128 GByte SD card for storing jpeg images (4608 × 3456 pixel). The camera can be externally triggered and has an electronic shutter. Compared to a mechanical shutter, the electronic shutter does not suffer from wear and is not affected by low temperatures. Furthermore, the focus of this camera model can be set manually and remains fixed during deployment, as the lens does not automatically retract on power-off. A microcontroller (Arduino Nano) is used to control the power supply to the camera and to trigger the image acquisition. In addition, we measure ambient light and suspend image acquisition during night, which helps to conserve energy and data storage space. The microcontroller can be programmed via USB to support

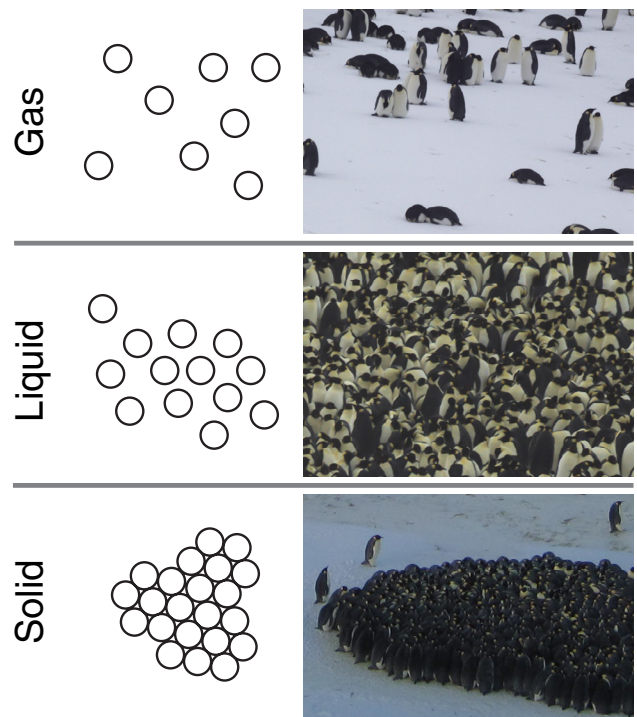


Figure 1. Comparison of phase (aggregation) states of non-living matter and states of emperor penguin colonies: In a gas-like state, individuals are loosely aggregated, and their motion is not impeded. In a liquid-like state, denser clusters without long-range order appear. In a solid-like state, individuals are arranged in a dense, quasi-hexagonal structure with long-range order, and individual motion becomes impossible.

frame rates of up to one image per second. The system is powered by a lithium ion battery (7.3 V, 20 Ah) that is recharged by two 20 W solar panels. During the Austral winter, the solar panels are insufficient, and the battery is exchanged together with the SD cards every 3 days.

The camera is mounted on a sturdy tripod, and the camera’s field of view can be adjusted to keep the moving colony in sight. The observatory can be carried by one person and can be erected in poorly accessible areas, e.g. on the rocky tips of the islands around Dumont d’Urville station.

Meteorological data, including air temperature, wind speed and wind direction, humidity and global solar radiation (the sum of direct and diffuse solar radiation) are acquired by the meteorological observatory (Météo France) at Dumont d’Urville (Ile des Pétrels, figures 2(a) and (b)). As the colony remains in close proximity to the base (less than 1000 m), these measurements are assumed to be representative for the conditions experienced by the colony.

Data preparation

We use the area covered by the colony as order parameter to quantify the state of the penguin colony. The minimum area corresponds to the highest density of the colony when all penguins are huddling (solid state), and the maximum area corresponds to the lowest density where nearly all penguins are scattered and only few, small huddling groups are present (liquid and/or gas state).

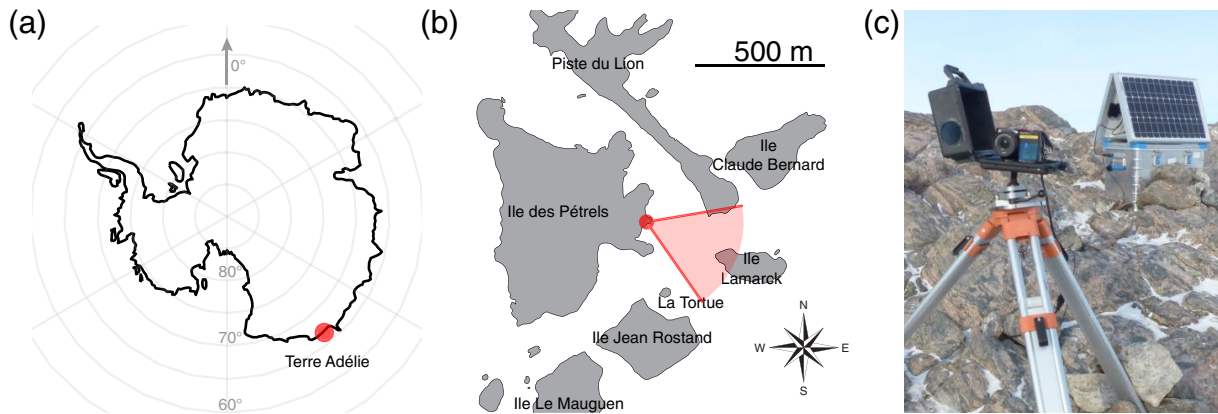


Figure 2. (a) position of the Pointe Géologie colony (b) position and field-of-view of the micrObs observatory. (c) The observatory is positioned on the rocky peaks of the surrounding islands for optimum viewing angle.

We limit our analysis to the time between mid-April and the end of May, a period with sufficient light to acquire low-noise time-lapse recordings over multiple hours, and varying environmental conditions where different phase states occur. Moreover, during this time period, we can assume that the influence of the breeding cycle on the penguins' huddling behaviour is minimal, because the animals just returned from several months of foraging and are well nourished. Also, there are no chicks present that could influence the huddling behaviour.

We selected only days for the analysis that fulfil the following conditions: good visibility over the whole day, and a quasi-stationary colony that predominantly remains in the field of view of the camera (figure 3(a)). Within the study period, we selected 8 out of 10 consecutive days (supplementary information table 1, supplementary figure S1 (stacks.iop.org/JPhysD/51/214002/mmedia)) that fulfil these criteria.

We extract the area occupied by the colony using an automatic image segmentation algorithm. The segmentation is based on an adaptive K-means clustering (Bradski, 2000) of pixel intensities (figure 3(b)). Pixel intensities are clustered into five groups. The group with the lowest mean intensity corresponds to the black plumage of the penguins. This approach proved to be robust to changes in illumination and shadows. To simplify the task, we manually masked rocks and heavily guano stained ground using ClickPoints (Gerum *et al* 2017a), and excluded them from the segmentation. One image every 3 min was analysed.

To correct for perspective distortions, we calculate the area represented by one pixel depending on its vertical (y -) position in the image. The calculation is based on the projection specified by the intrinsic and extrinsic camera matrix (supplementary figure S2, Gerum *et al* 2017b). The colony area is then calculated as the perspective-corrected area of the pixels belonging to the K-means group with the lowest intensity. We assume the number of penguins that are present within the field-of-view to be constant during the observed period. Therefore, we can normalize the colony area for the observed period by the maximum colony area across all evaluated days, after subtracting the absolute minimum colony area from

every data point. The normalized area A_{norm} therefore varies between zero and unity. If we were to observe the colony from directly above (nadir), the colony area as defined here would simply be the sum of the area occupied by each penguin and hence remain constant regardless of colony density. At shallower viewing angles, however, penguins standing in the front occlude penguins standing further behind, and thus the colony area decreases approximately linearly with increasing density (supplementary figure S3). If we further assume the co-existence of two phases (huddles versus loosely clustered or free standing penguins), with each phase having an approximately constant average density, the normalized area is also a measure of the inverse huddling probability of the colony, with zero corresponding to the situation where (nearly) all penguins are in a huddle, and unity corresponding to the situation where (nearly) all penguins are free-standing.

Three simplifications were necessary for the automated evaluation of colony area and huddling probability: First, we cannot differentiate between the white plumage and the sea ice, resulting in a trend to underestimate the area especially at low densities. Second, because of the occlusion effect, a large huddle has a somewhat smaller area compared to multiple smaller huddles with the same total number of huddling penguins. Third, if the density of the penguins in the fluid/gas phase changes over time, this will change the degree of occlusion and hence affect the colony area (supplementary figure S3).

To reduce noise in the measurements, colony area and meteorological data are smoothed along the time axis using a least squares smoothing filter (first order Savitzky–Golay filter over 15 data points, Savitzky and Golay 1964) corresponding to a smoothing over 45 minutes (see figure 3(e)).

Model

To prevent overfitting of the limited data available (8 d, 3000 data points), we choose a simple two-stage model. First, we assume that the huddling state (or phase) of penguins as expressed by the normalized colony area changes only in response to an apparent temperature T_a . Second, we assume

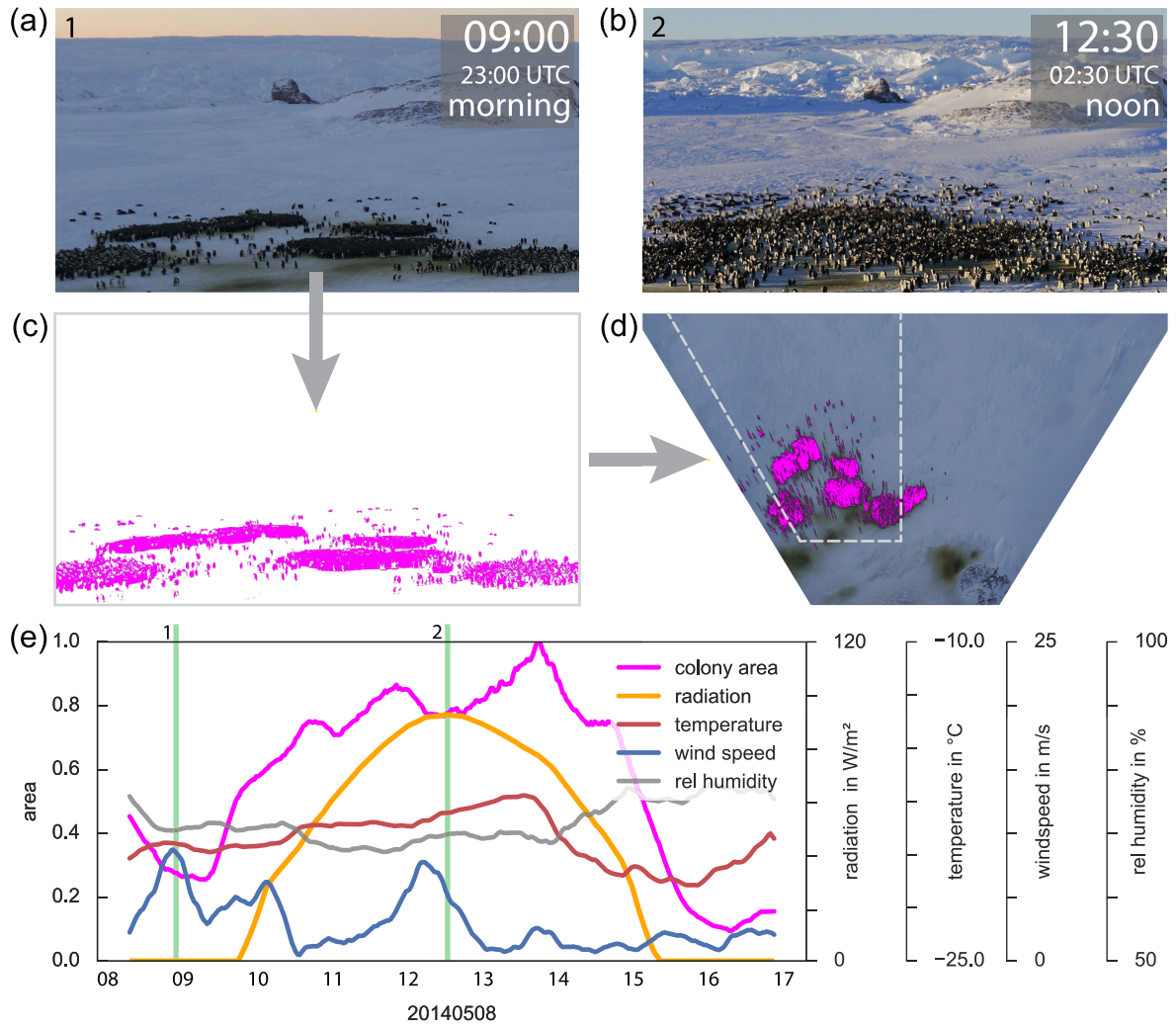


Figure 3. Images of the colony in the morning (a) and at noon (b); the change of the occupied area is clearly visible. The colony area is quantified based on a binary segmentation (c) followed by a correction of perspective image distortions (top-view projection) (d). Temporal fluctuations of normalized colony area (pink), temperature (red), wind speed (blue), global radiation (yellow) and humidity (grey) (e). See supplementary video SF1.

that the phase transition occurs as a monotonous function over a temperature range of T_a .

Apparent temperature. The apparent temperature T_a is expressed as a generalized linear model (equation (1)). Inspired by the wind chill factor for human temperature perception, the apparent temperature is defined as a combination of the environmental parameters ambient temperature (T), wind speed (W), global solar radiation (R) and relative humidity (H):

$$T_a = T + c_W W + c_R R + c_H H. \quad (1)$$

Except for ambient temperature T , all other environmental parameters are weighted by the model coefficients c_W (wind chill factor), c_R (solar heating factor) and c_H (humidity chill factor). We keep the apparent temperature dimensional ($^{\circ}\text{C}$) so that the contributions of the meteorological factors can be expressed in units of $^{\circ}\text{C}$ per unit of the changing parameter. For example, an increase in wind speed of 5 m s^{-1} is perceived as a temperature reduction by $14.3 \text{ }^{\circ}\text{C}$ (see results).

Phase transition. We suggest that the normalized area A_{norm} occupied by the colony represents the huddling state and thus the phase of the penguin colony, where 0 corresponds to tight huddling or solid state, and 1 corresponds to a loosely clustered or liquid/gas state. The phase transits smoothly between 0 and 1 over a range of apparent temperatures according to a sigmoid function:

$$A_{norm} = \frac{1}{(1 + e^{-(T_a + T_{trans})/b_0})}. \quad (2)$$

The phase transition point T_{trans} is the apparent temperature at which half of the penguins are in a huddle. The parameter b_0 denotes the apparent temperature range over which the phase transition occurs and hence defines the width of the sigmoid function.

Model training. The model parameters are determined using Bayesian inference, based on the probabilistic programming framework PyMC3 (v3.0) package for Python (Salvatier *et al*

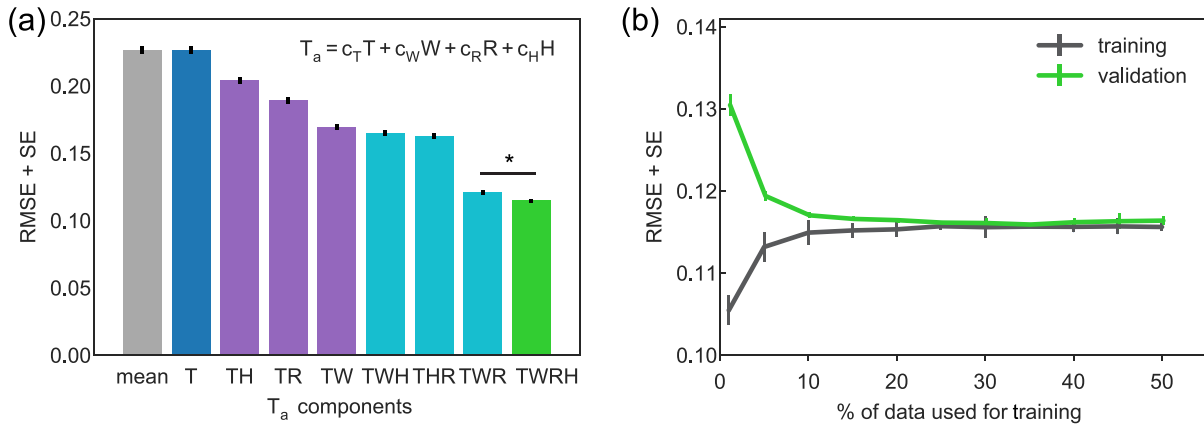


Figure 4. (a) root mean squared error (RMSE \pm sd) for the prediction of the trainings dataset, depending on the environmental variables (temperature T, humidity H, wind speed W, global solar radiation R) included in the model. Coefficients of unused variables are set to zero. The improvement of the TWRH model over the TWR model is significant ($p < 0.05$). (b) RMSE (mean \pm sd) of the model with 4 environmental parameters (TWRH) for training and independent validation dataset versus the percentage of data used for training. The standard error is calculated over all possible cross validation splits. The difference between training and validation error vanishes at 25%.

2015). In contrast to the classical frequentist approach, which provides a single value for each parameter, the Bayesian approach provides a parameter distribution, which is a direct measure of the uncertainty.

For model selection and parameter estimation, we use normally-distributed priors and a Metropolis-Hastings sampler (a Markov chain Monte Carlo method) to draw 100 000 samples to approximate the parameter distributions. We discard the first 10% of the samples (burn-in) to reduce the influence of the initial point estimate, which is used as a starting point for the sampling process. Predictions are drawn from the posterior parameter distributions and averaged over 1000 samples. For the final model, we draw $4 \cdot 10^6$ samples, discard the first 10^6 as burn-in and take every 10th sample to remove potential short-range autocorrelations that can occur as an artefact of the sampling process.

Model selection. To determine the importance of individual environmental parameters on the predictive performance of the model, we iteratively exclude parameters ($c_T = 1$; exhaustive combinations of c_W , c_R and c_H set to 0), and calculate the RMSE (root mean squared error) between the model prediction and the measured normalized colony area. We verify that we have sufficient data for the proposed model using a cross validation evaluation with increasing numbers of training samples. Data samples are considered sufficient when training and test error converge.

To quantify whether an additional parameter increases the model performance due to new information and not simply by increasing the degrees of freedom, we replace the value in question with a randomly sampled uniformly distributed variable and compare the model performance. Significance is tested using bootstrapping.

Predictive capability on the limited dataset is tested using a ‘leave one out’ training scheme (Hastie *et al* 2001), where the model is trained on $n-1$ of the n available sample days and is tested on the excluded day.

Results

Daily overview plots (figure 3(e) and supplementary figure S4) indicate a positive correlation between global radiation and the colony area, and a noticeable negative correlation with increasing wind speed. By contrast, daily changes in temperature and relative humidity are relatively small, and thus it is difficult to clearly discern a correlation with colony area. We do not consistently observe huddling below or above a threshold of any single meteorological variable.

We evaluate the effect of individual environmental parameters on the colony area by exhaustively iterating over all combinations and comparing the RMSE between the measured huddle area and the model (figure 4(a)). We find that ambient temperature (T, $\text{rmse} = 0.228$) alone does not significantly ($p > 0.05$) improve the fit of the model to the data compared to the simplest model of a constant mean colony area. This is because the temperature shows only small variations over the course of each of the investigated days (supplementary figure S4). When we combine temperature with a second environmental parameter, however, we find a significant ($p < 0.05$) improvement of the model. Especially the combination of temperature and wind speed lead to the best results for two environmental parameters (TW, $\text{rmse} = 0.169$), corresponding to a 25.6% improvement over a model with temperature as sole input variable. When we combine temperature with two parameters, we find a significant ($p < 0.05$) improvement only for the combination of temperature, wind speed and global radiation (TWR, $\text{rmse} = 0.121$) with a further improvement of 28.4% compared to temperature and wind speed (TW). Including humidity as a fourth parameter leads to further small but significant ($p < 0.05$) improvement (TWRH, $\text{rmse} = 0.115$) of 5.0% compared to the best model with three environmental parameters (TWR) (supplementary figure S5).

To verify that the model does not have too many degrees of freedom for the available amount of training data, we train the model on an increasing number of samples and evaluate

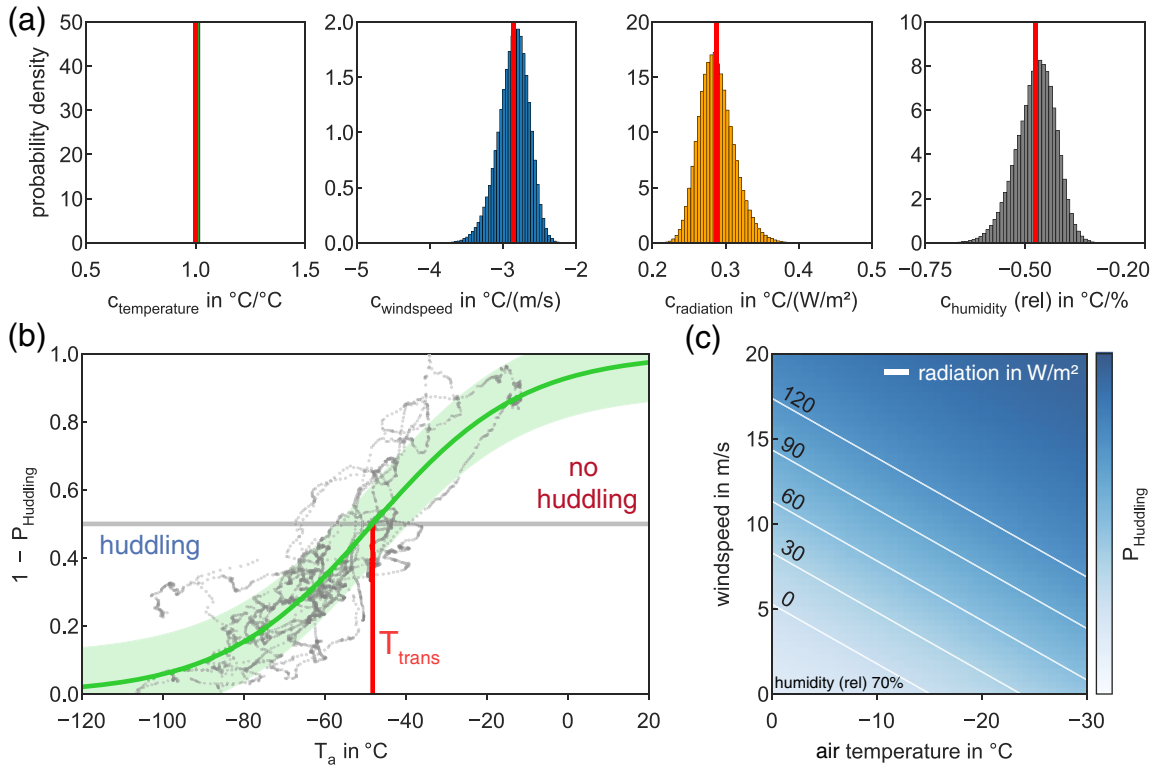


Figure 5. (a) distribution of model coefficients as estimated by Bayesian inference. The mean is shown by the red line. (b) Normalized colony area (corresponding to the inverse huddling probability) versus apparent temperature. Grey dots show the data from 8 days. The green line shows the model according to equation (2). Green shaded area indicates the standard deviation of the model. The red line indicates the apparent transition temperature T_{trans} where the huddling probability is 0.5. (c) Phase transition diagram for a fixed air humidity (70%). Lines of equal huddling probability ($p = 0.5$) for different solar radiation in a wind speed versus temperature diagram. Points with wind speeds and temperatures above the line have a huddling probability $p > 0.5$ as indicated by the blue shading.

the training and validation error (figure 4(b)). With less than 15% of the dataset used for training, we observe a large difference between the error of the training and validation dataset, indicating overfitting (a low error on the training data, but a larger error on the validation data indicates poor generalization). When more than 25% of the data set is used for training, however, the training and validation errors converge, indicating good generalisation and saturation of the model. We also performed a ‘leave one out’ evaluation where we train the model on the data from 7 d and validate the model on the remaining day for all possible combinations (see supplementary figures S6 and S7). This results in a mean RMSE of 0.115 ± 0.004 for the training data and 0.138 ± 0.043 for the validation data, demonstrating the predictive power of the model.

To determine the final model parameters ($c_T, c_W, c_R, c_H, T_{trans}, b_0$, see equations (1) and (2)), we sample the posterior distributions for the full dataset. Resulting parameter distributions are shown in figure 5(a) and table 1, the Bayesian sampling trace plot is shown in supplementary figure S8.

We set the temperature coefficient c_T to 1, which allows us to interpret all other coefficients as conversion factors towards an apparent temperature. The wind chill factor indicates a reduction in apparent temperature of $c_W = -2.857$ °C per

Table 1. Model parameters based on the full dataset.

	c_T	c_W	c_R	c_H	b_0	T_{trans}
Unit	—	°C (ms ⁻¹) ⁻¹	°C (Wm ⁻²) ⁻¹	°C/%	°C	°C
Mean	1	-2.857	0.288	-0.473	18.650	-48.167
Std	0	0.212	0.024	0.050	1.536	3.213
CV ($\frac{\sigma}{ \mu }$)	—	0.074	0.083	0.106	0.082	0.067

1 m s^{-1} wind speed increase. The solar heating factor indicates an increase in apparent temperature of $c_R = 0.288$ °C per W m^{-2} of global solar radiation. The humidity chill factor indicates a reduction in apparent temperature of $c_H = -0.473$ °C per % in relative air humidity. The coefficient of variation for these parameters (table 1 and figure 5(a)) agrees with our assessment from the model selection that key parameters are in the order wind speed, radiation, humidity (figure 4(a)).

Our model describes a transition from a solid to a liquid/gas state of the colony over a broad range ($b_0 = 18.65$ °C) of apparent temperatures (figure 5(b)), with a phase transition temperature of -48.167 °C where the probability is equal for both states. We can visualize the huddling probability in a phase transition diagram as shown in figure 5(c).

Discussion

In this report, we show that the huddling behaviour of emperor penguins can be described as a phase transition that is dependent on at least 4 environmental parameters: ambient temperature, wind speed, global solar radiation, and relative humidity. Using a linear combination of these environmental parameters, motivated by the concept of the wind-chill factor (Ames and Insley 1975, Siple and Passel 1999), we find an apparent temperature that controls the phase state of the colony. Moreover, we find that the transition from a high-density solid-like state (huddling) to a low density liquid/gas-like state (dispersed) occurs over a broad range of apparent temperatures.

Our findings are in agreement with the well-established notion that the primary purpose of emperor penguin huddling is to conserve energy and not, for example, a mechanism to protect against predators (Le Maho 1977). A previous study reported that average colony density was correlated with ambient temperature but not with wind speed (Gilbert *et al* 2008). Further experiments were performed with data loggers in combination with video recordings to investigate the influence of environmental parameters on the number of huddles and the mean number of individuals per huddle (Ancel *et al* 2015). This study reported a significant correlation of both measures with temperature, wind speed and radiation, but not with humidity. The correlation values, however, cannot be directly compared with our parameters as the huddling probability that we report is a combination of both, huddle number and number of individuals per huddle. Results of both previous studies are summarized in supplementary information table 2.

Based on measurements of the huddling probability extracted from time-lapse images, we have quantified the contribution of the following environmental parameters: ambient temperature, wind speed, global solar radiation, and relative humidity. We show that fluctuations of the huddling state cannot be explained by fluctuations of the ambient temperature alone. This is largely explained by the small temperature variations of ± 5.0 °C over the course of 8 days (see supplementary figure S9), and less than ± 3.0 °C over the course of any given day (see supplementary figure S4). By including additional environmental parameters, the model improves significantly. With four environmental parameters and two additional parameters describing the sigmoid shape of the apparent temperature range over which the phase transition process from a densely packed huddle to a loosely packed configuration occurs, we can account for approximately 50.7% of the huddling probability fluctuations. The remaining fluctuations that are not captured by our model are likely the result of physiological and behavioural processes. For example, even at low apparent temperatures, individual huddles might break up after exceeding an average lifetime of 1.6 h (SD = 1.7 h) (Gilbert *et al* 2006), which is thought to be triggered by individual penguins in a huddle that have sufficiently warmed up. This behaviour could be included in the model by tracking individual animals in the image data and thus considering their past huddling history. With the data presented here, tracking of individual penguins inside a

huddle is impossible due to limited spatial and temporal resolution. Recent developments (Richter *et al* 2018) will provide a more suitable data basis for this analysis. We also tested if the model predictions can be further improved by introducing a time-delayed huddling response of up to 6 h to account for thermal inertia or physiological adaptation, but this did not lead to significant improvements (data not shown).

Most of the time, the penguin colony shows coexistence of solid phases (huddles) and liquid/gas phases (loosely packed or free-standing penguins). Thus, the phase transition from a solid to a liquid/gas state does not occur at a sharp apparent temperature. Instead, we find a sigmoidal relationship between huddling probability and apparent temperature, whereby the huddling probability decreases from 1 to 0 over an apparent temperature range of 140 °C, with a transition temperature of -48.2 °C at which the coexistence of solid and liquid/gas states is equally likely. The broad temperature range over which the phase transition occurs within the colony may be a combined effect of different transition temperatures for different individuals, a wide distribution of current skin temperatures among different individuals due to their individual huddling history and body constitution, or an oversimplification of our estimate of the apparent temperature as a linear combination of environmental parameters. Moreover, broadening of the temperature range over which the phase transition occurs may be caused by differences between the measured environmental conditions at the meteorological station and the colony site which is up to 1 km away. In particular westerly winds may be partially shielded by the close-by ~ 40 m high elevations of the Île des Pétrels, but since the dominant (76.9%) wind direction is easterly (45° – 135°) where elevations reach maximally 22 m and are further (~ 300 m) away (figure 3(a), supplementary figure S10), we do not expect this to be a major confounding factor.

Despite these limitations, we propose that the model parameters, in particular the phase transition temperature, are indicators of the colony's energy budget/reserves. Physiological changes that naturally occur over the course of the breeding cycle (e.g. diminishing energy reserves and reduction in fat insulation, or the presence of chicks) will necessarily change the temperature perception and huddling behaviour (Robin *et al* 1998, Groscolas and Robin 2001, Ancel *et al* 2015), and hence the parameters of our model are valid only for the time span over which the training data was acquired. By continuously updating the training data over the course of the incubation part of the breeding season, we suggest that the time evolution of the model parameters, in particular the phase transition temperature T_{trans} , report the seasonal energy budget of the colony and may therefore help to predict colony foraging efficiency that will affect the breeding success of the population. Moreover, by monitoring these parameters over multiple years, we may gain a better understanding of how climatic changes or altered food supply may impact the foraging success reflected in the colony's energy reserves, and ultimately population dynamics (Jenouvrier *et al* 2014). Given the simplicity of the model and the ease with which huddling statistics can be automatically acquired using remote-controlled or autonomous observatories (Richter *et al* 2018), we believe

that our method has the potential to become a valuable tool for large-scale colony monitoring.

Acknowledgments

This study was funded by the Deutsche Forschungsgemeinschaft (DFG) grants FA336/5-1 and ZI1525/3-1 in the framework of the priority program ‘Antarctic research with comparative investigations in Arctic ice areas’. This work was supported by the Postdoctoral Scholar Program at the Woods Hole Oceanographic Institution, with funding provided by the Doherty Foundation, by NIH Grant HL65960 and was conducted within the framework of the Programme 137 of the Institut Polaire Français Paul-Emile Victor (IPEV), with additional support from the Centre Scientifique de Monaco through budget allocated to the Laboratoire International Associé 647 BioSensib (CSM/CNRS-University of Strasbourg), the Centre National de la Recherche Scientifique (Programme Zone Atelier de Recherches sur l’Environnement Antarctique et Subantarctique). We thank IPEV Logistics and the winterers at Dumont d’Urville for their invaluable support, and Météo France for the meteorological data of Dumont d’Urville. The authors declare no competing interests.

ORCID iDs

S Richter  <https://orcid.org/0000-0002-1948-7088>
 R Gerum  <https://orcid.org/0000-0001-5893-2650>
 A Winterl  <https://orcid.org/0000-0003-0688-9317>
 B Fabry  <https://orcid.org/0000-0003-1737-0465>
 D P Zitterbart  <https://orcid.org/0000-0001-9429-4350>

References

- Ames D R and Insley L W 1975 Wind-chill effects for cattle and sheep *J. Animal Sci.* **40** 161–5
- Ancel A, Gilbert C, Poulin N, Beaulieu M and Thierry B 2015 New insights into the huddling dynamics of emperor penguins *Animal Behav.* **110** 91–8
- Bradski G 2000 The openCV library *Dr. Dobb's J. Softw. Tools* **25** 120–5
- Canals M and Bozinovic F 2011 Huddling behavior as critical phase transition triggered by low temperatures *Complexity* **17** 35–43
- Gerum R, Fabry B, Metzner C, Beaulieu M, Ancel A and Zitterbart D P 2013 The origin of traveling waves in an emperor penguin huddle *New J. Phys.* **15** 125022
- Gerum R, Richter S, Fabry B and Zitterbart D P 2017a ClickPoints: an expandable toolbox for scientific image annotation and analysis *Methods Ecol. Evol.* **8** 750–6
- Gerum R, Richter S, Winterl A, Fabry B and Zitterbart D P 2017b Cameratransform: a scientific python package for perspective camera corrections (arXiv:1712.07438)
- Gilbert C, McCafferty D, Le Maho Y, Martrette J M, Giroud S, Blanc S and Ancel A 2010 One for all and all for one: the energetic benefits of huddling in endotherms *Biol. Rev.* **85** 545–69
- Gilbert C, Robertson G, Le Maho Y and Ancel A 2008 How do weather conditions affect the huddling behaviour of emperor penguins? *Polar Biol.* **31** 163–9
- Gilbert C, Robertson G, Le Maho Y, Naito Y and Ancel A 2006 Huddling behavior in emperor penguins: dynamics of huddling *Physiol. Behav.* **88** 479–88
- Groscolas R and Robin J-P 2001 Long-term fasting and re-feeding in penguins *Comp. Biochem. Physiol. A* **128** 643–53
- Hastie T, Tibshirani R and Friedman J 2001 The elements of statistical learning *Math. Intell.* **27** 83–5
- Isenmann P 1971 Contribution à l'éthologie et à l'écologie du manchot empereur (*aptenodytes forsteri gray*) à la colonie de pointe géologie (terre adélie) *Oiseau Rev. Fr. Ornithol.* **41** 9–64
- Jenouvrier S, Holland M, Stroeve J, Serreze M, Barbraud C, Weimerskirch H and Caswell H 2014 Projected continent-wide declines of the emperor penguin under climate change *Nat. Clim. Change* **4** 715–8
- Le Maho Y 1977 The emperor penguin: a strategy to live and breed in the cold: morphology, physiology, ecology, and behavior distinguish the polar emperor penguin from other penguin species, particularly from its close relative, the king penguin *Am. Sci.* **65** 680–93
- Prévost A 1961 *Ecologie du Manchot Empereur, Expéditions Polaires Françaises.* (Paris: Hermann)
- Richter S, Gerum R C, Schneider W, Fabry B, Le Bohec C and Zitterbart D P 2018 A remote-controlled observatory for behavioural and ecological research: a case study on emperor penguins *Methods Ecol. Evol.* **00** 1–11
- Robin J-P, Boucontet L, Chillet P and Groscolas R 1998 Behavioral changes in fasting emperor penguins: evidence for a ‘refeeding signal’ linked to a metabolic shift *Am. J. Physiol.* **274** R746–53
- Salvatier J, Wiecki T and Fonnesbeck C 2015 Probabilistic programming in python using PyMC *PeerJ Comput. Sci.* **2** e55
- Savitzky A and Golay M J E 1964 Smoothing and differentiation of data by simplified least squares procedures *Anal. Chem.* **36** 1627–39
- Siple M P A. and Passel C F 1999 Excerpts from: measurements of dry atmospheric cooling in subfreezing temperatures *Wilderness Environ. Med.* **10** 176–82
- Vicsek T and Zafeiris A 2012 Collective motion *Phys. Rep.* **517** 71–140
- Zitterbart D P, Wienecke B, Butler J P and Fabry B 2011 Coordinated movements prevent jamming in an emperor penguin huddle *PLoS One* **6** e20260